A Thesis for the degree of Doctor of Philosophy

Therapeutic effect of alendronate in spinal cord injury

Department of Veterinary Medicine

GRADUATE SCHOOL

JEJU NATIONAL UNIVERSITY

Yuna Choi

2021. 8.

Therapeutic effect of alendronate in spinal cord injury

Yuna Choi
(Supervised by Professor Taekyun Shin)

A thesis submitted in partial fulfillment of the requirement for the degree of Doctor of Philosophy in Veterinary Medicine

2021. 8.

This thesis has been examined and approved.

.....
Thesis director, Jeongtae Kim, Ph.D., Kosin University

.....
Kyungsook Jung, Ph.D., Korea Research Institute of Bioscience and Biotechnology

.....
Meejung Ahn, Ph.D., Sangji University

.....
Hyun Ju Ko, Ph.D., Coseed Biopharm

.....
Taekyun Shin, Ph.D., Jeju National University

.....

Department of Veterinary Medicine
GRADUATE SCHOOL
JEJU NATIONAL UNIVERSITY

CONTENTS

List of Abbreviations

CGRP	calcitonin gene-related peptide
ChAT	choline acetyltransferase
COX-2	cyclooxygenase-2
D	days
ERK1/2	extracellular signal-regulated kinase1/2
GAPDH	glyceraldehyde 3-phosphate dehydrogenase
GFAP	glial fibrillary acidic protein
Iba1	ionized calcium-binding adapter molecule 1
IL-1β	interleukin-1 beta
JNK1/2	c-jun-NH_2-terminal kinase1/2
KCC2	potassium chloride co-transporter 2
MAPK	mitogen-activated protein kinase
NIH	National Institutes of Health
PBS	phosphate-buffered saline
PCR	polymerase chain reaction
p-ERK1/2	phosphorylated form of extracellular signal-regulated kinase1/2
PI	post-injury
p-JNK1/2	phosphorylated form of c-jun-NH_2-terminal kinase1/2
p-p38	phosphorylated form of p38
SCI	spinal cord injury
Serpina3n	serine peptidase inhibitor, clade A, member 3N
TNF-α	tumor necrosis factor-alpha

List of Figures

List of Tables

Therapeutic effect of alendronate in spinal cord injury

1. Abstract

Spinal cord injury is a destructive disease characterized by motor/sensory dysfunction and severe inflammation. Alendronate is an anti-inflammatory and may therefore be of benefit in the treatment of the inflammation associated with spinal cord injury. This study aimed to evaluate whether alendronate attenuates motor/sensory dysfunction and the inflammatory response in a thoracic spinal cord clip injury model. Alendronate was intraperitoneally administered at 1 mg/kg/day from day (D) 0 to 28 post-injury (PI). The histopathological evaluation showed an alleviation of the inflammatory response, including the infiltration of inflammatory cells, and a decrease in gliosis. Alendronate also led to reductions in the levels of inflammation-related molecules, including mitogen-activated protein kinase, p53, pro-inflammatory cytokines, and pro-inflammatory mediators. Immunohistochemical staining using calcitonin gene-related peptide, choline acetyltransferase, and potassium chloride co-transporter 2 indicated that alendronate promoted axonal regeneration. Neuro-behavioral assessments, including the Basso, Beattie, and Bresnahan scale for locomotor function, the von Frey filament test, the hot plate test, and the cold stimulation test for sensory function, and the horizontal ladder test for sensorimotor function improved significantly in the alendronate-treated group at D28PI. Taken together, these results suggest that alendronate treatment can inhibit the inflammatory response in spinal cord injury and promote axonal regeneration, thus improving functional responses.

Key words: Alendronate, Axonal regeneration, Behavioral test, Inflammation, Spinal cord injury.

2. Introduction

Spinal cord injury (SCI), including contusion, transection and compression, is accompanied by secondary degeneration, autonomic dysfunction and an inflammatory response (Heo et al., 2020). The severity of the paralysis resulting from SCI differs by site (Ahmed et al., 2019). Thoracic clip compression injury is a reproducible method for studying hind-limb paralysis (Kjell and Olson, 2016) as it reproduces the severe inflammatory response in the spinal cord, characterized by the infiltration of inflammatory cells, microgliosis, and astrogliosis (Heo et al., 2020, Kim et al., 2003). Mitogen-activated protein kinase (MAPK) signaling, such as extracellular signal-regulated kinase (ERK), c-jun-NH2-terminal kinase (JNK), and p38, is activated after SCI and activation occurs in parallel with the stimulation of pro-inflammatory cytokines (Martini et al., 2016). Among the therapeutic targets of SCI are a reduction of the secondary damage, stem cell replacement therapy, the removal of inhibitory molecules, promotion of the regenerative response, and improvement of axonal growth, remyelination, and rehabilitation (Griffin and Bradke, 2020). The most common therapeutic target of SCI is a reduction of the secondary damage using neuro-protective or anti-inflammatory molecules.

Alendronate is a nitrogen-containing bisphosphonate that can cross the blood-brain barrier (Oliveira and Oliveira, 2016) and is widely used to treat osteoporosis (Sharpe et al., 2001). Alendronate regulates farnesyl pyrophosphate and geranylgeranyl pyrophosphate synthesis in the mevalonate pathway (Tricarico et al., 2015). Some recent clinical trials suggested that alendronate relieves pain, non-steroidal anti-inflammatory drug resistance, and stiffness, and improves the movement of affected joints (Nishii et al.,

2013). Decreased cholesterol synthesis after alendronate crosses the blood-brain barrier has also been shown in a rat model of Alzheimer's disease (Zameer et al., 2018). The anti-inflammatory effect of alendronate, demonstrated in experimental autoimmune encephalomyelitis, an animal model of human multiple sclerosis, occurs through a decrease in infiltration of inflammatory cells and pro-inflammatory cytokines, including interleukin-1 beta (IL-1β), tumor necrosis factor-alpha (TNF-α), and interferon-gamma (Jung et al., 2020). The serine peptidase inhibitor, clade A, member 3N (Serpina3n), is an essential neuroinflammation-dependent molecule associated with trimethyltin chloride-induced neurotoxicity (Xi et al., 2019) and localized in the reactive astrocytes in Alzheimer's disease (Abraham, 2001). Serpina3n is regulated in a model of ischemia-reperfusion injury model induced by minocycline treatment (Abcouwer et al., 2013). However, the effect of alendronate on central nervous system diseases, including SCI, requires further study.

Thus, this study evaluated the effect of alendronate on SCI, and the underlying mechanism based on histopathological and behavioral tests.

3. Materials and Methods

3.1. Animals

Female Sprague-Dawley rats (6–7 weeks old; Samtako, Gyeonggi-do, Korea) were maintained in our facility under normal conditions (12-h light/dark cycle, temperature = 23 ± 2°C). All animal protocols conformed to international laws and National Institutes of Health (NIH) policies, including the Care and Use of Laboratory Animals (NIH publication no. 85-23, 1985, revised 1996). All experimental procedures were performed according to the Guidelines for the Care and Use of Laboratory Animals of Jeju National University (permission number: 2021-0009).

3.2. Experimental groups and procedure

Clip compression injury was induced as in our previous studies (Ahn et al., 2012). Briefly, the rats were anesthetized with Zoletil® 50 (0.2 ml/animal, Virbac, Carros, France) and laminectomized at the spinous process of the tenth thoracic vertebra. The exposed thoracic spinal cord was compressed horizontally using a 35–55 g vascular clip (00466; S&T®, Rheinfall, Switzerland) for 1 min (Fig. 1). Thereafter, the surgical site, including the muscle and skin layers, were sutured. The rats were classified into five groups to investigate the effect of alendronate on SCI: normal control (n = 10), sham control (n = 10), SCI + vehicle-treated (n = 10), SCI + alendronate 1 mg/kg-treated (n = 10) and SCI + alendronate 5 mg/kg-treated (n = 10). Alendronate was administrated intraperitoneally to SCI rats from day (D) 0 post-injury (PI) to D28PI (Y0001727; 1 mg/kg/day or 5 mg/kg/day; EDQM, Strasbourg, France) (Yao et al., 2016) (Fig. 2).

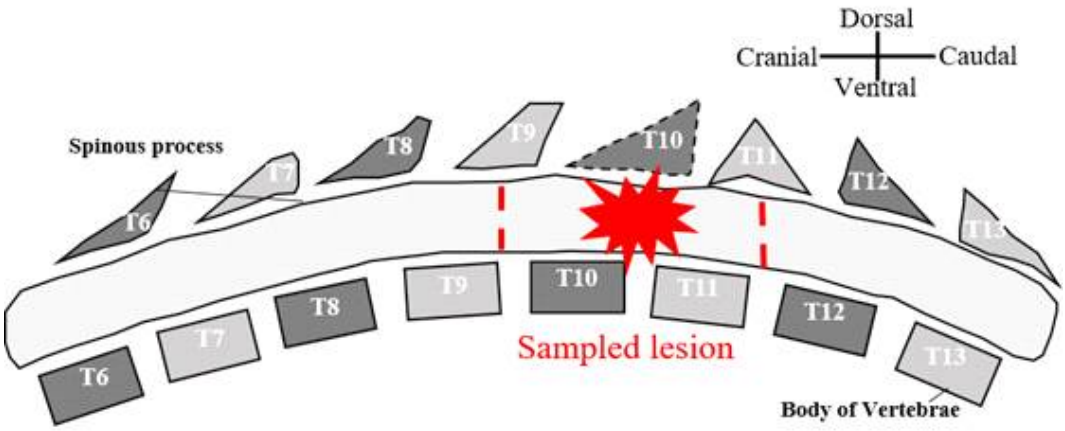

Figure 1. Compression site of spinal cord. T, thoracic vertebrae.

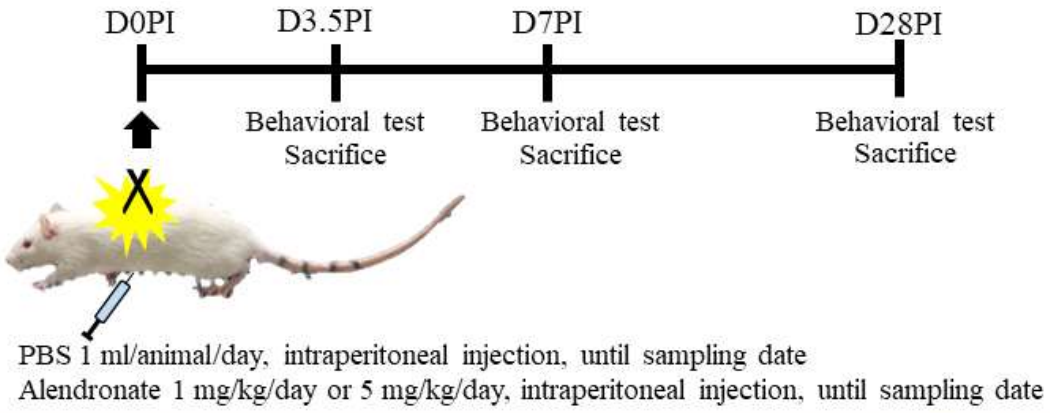

Figure 2. The experimental schedule of alendronate treatment.

3.3. Tissue preparation

The rats were killed with CO_2 gas on D3.5PI, D7PI, and D28PI. Thoracic spinal cord samples (T9–T11) were obtained and fixed in 4% paraformaldehyde for histopathological examination. The samples were stored at −80°C until western blotting and real time-polymerase chain reaction (PCR) analysis.

3.4. Histological examination

The fixed tissues were embedded in paraffin wax and sectioned to 5-μm-thickness with a microtome (RM 2135; Leica, Nussloch, Germany). After deparaffinization, the sections were stained with hematoxylin and eosin.

3.5. Immunohistochemistry

The same immunohistochemistry protocol used in our previous study was performed (Choi et al., 2020). In brief, the sections were incubated with the primary antibodies listed in Table 1 for 1 h at room temperature. The matched secondary antibodies were reacted to the slides based on the primary antibody. An avidin-biotin complex kit (Vectastain Elite ABC Kit; Vector Laboratories) was applied. A 3-3′-diaminobenzidine substrate kit (Vector Laboratories, Burlingame, CA, USA) was used to visualize the peroxidase reaction, and the sections were counterstained with hematoxylin.

3.6. Western blot analysis

The western blot analysis proceeded according to our previous studies (Choi et al., 2020). The primary antibodies are listed in Table 1. The

primary antibody was reacted with horseradish peroxidase anti-mouse IgG (PI-2000, Vector Labs, Burlingame, CA, USA) or anti-rabbit IgG (PI-1000, Vector Labs, Burlingame, CA, USA) on the membrane overnight at 4℃. Enhanced chemiluminescence substrate (BS ECL Plus Kit, W6002; Biosesang, Gyeonggi, Korea) was used to visualize the immunoblot signals, which were quantified using Solo 6X and FUSION software (Vilber Lourmat, Collégien, France). The values of each immunoblot were normalized to β-actin.

Table 1. The characterization of antibodies

Antigen	Manufacturer, species, antibody type	Dilution
β-actin	Sigma Aldrich (a5441), mouse, monoclonal	1:10,000
CGRP	Sigma Aldrich (C8198), rabbit, polyclonal	1:50,000
ChAT	Millipore (AB144), goat, polyclonal	1:1,000
ED1	Bio-rad (MCA341), mouse, monoclonal	1:800
ERK1/2	Cell Signaling Technology (#4695), rabbit, monoclonal	1:1,000
GFAP	Sigma Aldrich (G3893), mouse, monoclonal	1:1,000
Iba1	WAKO (019-19741), rabbit, polyclonal	1:1,000
JNK1/2	Cell Signaling Technology (#9252), rabbit, polyclonal	1:1,000
KCC2	Original antibody, rabbit, polyclonal, (Kosaka et al., 2020)	1:100
p38	Santa Cruz Biotechnology (sc-535), rabbit, polyclonal	1:1,000
p53	Calbiochem (#OP03L), mouse, monoclonal	1:1,000
p-ERK1/2	Cell Signaling Technology (#4370), rabbit, monoclonal	1:1,000
p-JNK1/2	Cell Signaling Technology (#9251), rabbit, polyclonal	1:1,000
p-p38	Santa Cruz Biotechnology (sc-7973), mouse, polyclonal	1:1,000

Abbreviations: CGRP, calcitonin gene-related peptide; ChAT, choline acetyltransferase; ERK1/2, extracellular signal-regulated kinase1/2; GFAP, glial fibrillary acidic protein; Iba1, ionized calcium-binding adapter molecule 1; JNK1/2, c-jun-NH_2-terminal kinase1/2; KCC2, potassium chloride co-transporter 2; p-ERK1/2, phosphorylated form of extracellular signal-regulated kinase1/2; p-JNK1/2, phosphorylated form of c-jun-NH_2-terminal kinase1/2; p-p38, phosphorylated form of p38.

3.7. Real time PCR

Total RNA of the spinal cord in all groups (n = 6 per group) was extracted using TRIzol RNA Isolation Reagent (Life Technologies, Carlsbad, CA, USA). The cDNA was transcribed from purified RNA using the 5× First Strand cDNA Synthesis Master Mix (CellSafe, Gyeonggi-do, Korea). The PCR was performed with the minimum inhibitory concentration using the mic instrument (Bio Molecular Systems, Potts Point, Australia) and 2× Quantity SYBR Green (PhileKorea Co., Ltd., Seoul, Korea) as follows: 55 cycles of denaturation (10 s, 95°C), annealing (10 s, 60°C), and extension (10 s, 72°C). The Serpina3n primer (qRnoCID0005765, BioRad, CA, USA) and other primer sequences are summarized in Table 2.

Table 2 The primer sequences

Primer	Forward sequence	Reverse sequence
COX-2	5′-CGG AGG AGA AGT GGG GTT TA-3′	5′-TGG GAT GCA CTT GCG TTC AT-3′
GAPDH	5′-GGG GGC TCT CTG CTC CTC CC-3′	5′-CGG CCA AAT CCG TTC ACA CCG-3′
IL-1β	5′-CCC TGC AGC TGG AGA GTG TGG-3′	5′-TGT GCT CTG CTT GAG AGG TGC-3′
TNF-α	5′-CGT CGT AGC AAA CCA CCA AG-3′	5′-CAC AGA GCA ATG ACT CCA AA-3′

Abbreviations: COX-2, cyclooxygenase-2; GAPDH, glyceraldehyde 3-phosphate dehydrogenase; IL-1β, interleukin-1 beta; TNF-α, tumor necrosis factor-alpha.

3.8. Behavioral test

Locomotor function after SCI was evaluated using the Basso, Beattie, and Bresnahan rating scale (Basso et al., 1995). The scoring system is shown in Table 3. Sensory function was evaluated using the von Frey filament test (Gonzalez-Cano et al., 2018), in which a positive or negative response depends on the filament force. The results were calculated as the 50% threshold gram according to the following equation:

$$10^{X_f+\kappa\delta}/10{,}000$$

where X_f, value (in log units) is the final von Frey filament used, κ, is the tabular value of the pattern of positive/negative responses, and δ is mean difference (in log units) between stimuli.

The hot plate test (Gale et al., 1985) and the cold stimulation test using acetone (Deuis et al., 2017) were used to measure the latency of hind limb avoidance to hot or cold stimuli. Sensorimotor function was comprehensively evaluated in a horizontal ladder test (Metz and Whishaw, 2002) and rated from 0 to 6 (0, total miss; 1, deep slip; 2, slight slip; 3, replacement; 4, correction; 5, partial placement; and 6, correct placement). The behavioral tests were conducted in a double-blinded manner until D28PI. Spinal cord samples were obtained after the behavioral tests.

Table 3 The Basso, Beattie, and Bresnahan locomotor rating scale (Basso et al., 1995)

Scale	Characteristics
0	No Observable hindlimb movement
1	Slight movement of one or two joints, usually the hip and/or knee
2	Extensive movement of one joint or extensive movement of one joint and slight movement of one other joint
3	Extensive movement of two joints
4	Slight movement of all three joints of the hindlimb
5	Slight movement of two joints and extensive movement of the third
6	Extensive movement of two joints and slight movement of the third
7	Extensive movement of all three joints of the hindlimb
8	Sweeping with no weight support or plantar placement of the paw with no weight support
9	Plantar placement of the paw with weight support in stance only (i.e., when stationary) or occasional, frequent, or consistent weight supported dorsal stepping and no plantar stepping
10	Occasional weight supported plantar steps, no forelimb-hindlimb coordination
11	Frequent to consistent weight supported plantar steps and no forelimb-hindlimb coordination
12	Frequent to consistent weight supported plantar steps and occasional forelimb-hindlimb coordination
13	Frequent to consistent weight supported plantar steps and frequent forelimb-hindlimb coordination
14	Consistent weight supported plantar steps, consistent forelimb-hindlimb coordination; and predominant paw position during locomotion is rotated (internally or externally) when it makes initial contact with the surface as well as just before it is lifted off at the end of stance of frequent plantar stepping, consistent forelimb-hindlimb coordination, and occasional dorsal stepping
15	Consistent plantar stepping and consistent forelimb-hindlimb coordination; and no toe clearance or occasional toe clearance during forward limb advancement; predominant paw position is parallel to the body at initial contact
16	Consistent plantar stepping and consistent forelimb-hindlimb coordination during gait; and toe clearance occurs frequently during forward limb advancement; predominant paw position is parallel at initial contact and rotated at lift off
17	Consistent plantar stepping and consistent forelimb-hindlimb coordination during gait; and toe clearance occurs frequently during forward limb advancement; predominant paw position is parallel at initial contact and lift off
18	Consistent plantar stepping and consistent forelimb-hindlimb coordination during gait; and toe clearance occurs consistently during forward limb advancement; predominant paw position is parallel at initial contact and rotated at lift off
19	Consistent plantar stepping and consistent forelimb-hindlimb coordination during gait; and toe clearance occurs consistently during forward limb advancement; predominant paw position is parallel at initial contact and lift off and tail is down part or all of the time
20	Consistent plantar stepping and consistent coordinated gait; consistent toe clearance; predominant paw position is parallel at initial contact and lift off; tail consistently up; and trunk instability
21	Consistent plantar stepping and coordinated gait; consistent toe clearance; predominant paw position is parallel throughout stance; consistent trunk stability; tail consistently up

3.9. Statistical analysis

All values analyzed were mean ± standard error of three independent experiments. The results were analyzed using one-way analysis of variance followed by Student–Newman–Keuls post-hoc test for multiple comparisons. A p-value < 0.05 was considered significant. Three different sections from each rat ($n = 3$ animals/group) were analyzed and the percentage of stained area [(positive area/total area) × 100 (%)] was calculated. The total area included all layers of the spinal cord.

4. Results

4.1. Alendronate improved locomotor and sensorimotor function

The Basso, Beattie, and Bresnahan score was calculated daily from D0PI. The SCI rats exhibited significant deficits in locomotor function during the experiment. However, recovery of locomotor function was confirmed by an increase in the score from D10PI in the SCI + alendronate 1 mg/kg-treated group. The score tended to increase until D28PI in the SCI + alendronate 1 mg/kg-treated group, relative to that of the SCI + vehicle-treated group (Fig. 3A). Sensory, including thermal and mechanical, and sensorimotor function were tested before sampling. The hot plate and cold stimulation tests were used to examine thermal sensitivity (Fig. 3B and Fig. 3C). A loss of temperature sensitivity was detected at D3.5PI and D7PI in the SCI rats. Significant deficits remained in the SCI + vehicle-treated group on D28PI, whereas the latency of recognition of hot and cold had recovered in the SCI + alendronate 1 mg/kg-treated group. The von Frey filaments of varying thickness were used to assess the sensitivity to mechanical stimuli (Fig. 3D). The SCI rats showed significantly less responsivity, compared to the normal and sham control until the end of the experiment. However, the SCI + alendronate 1 mg/kg-treated group showed higher sensitivity in terms of the 50% paw withdrawal threshold than the SCI + vehicle-treated group. The horizontal ladder test was carried out pre-SCI and on the sampling date (Fig. 3E). Pre-SCI, the rats received high scores. The SCI rats, which were paralyzed in the hind limbs, were unable to cross the horizontal ladder without error, while the SCI + alendronate 1 mg/kg-treated group had better gait performance than the SCI + vehicle-treated group.

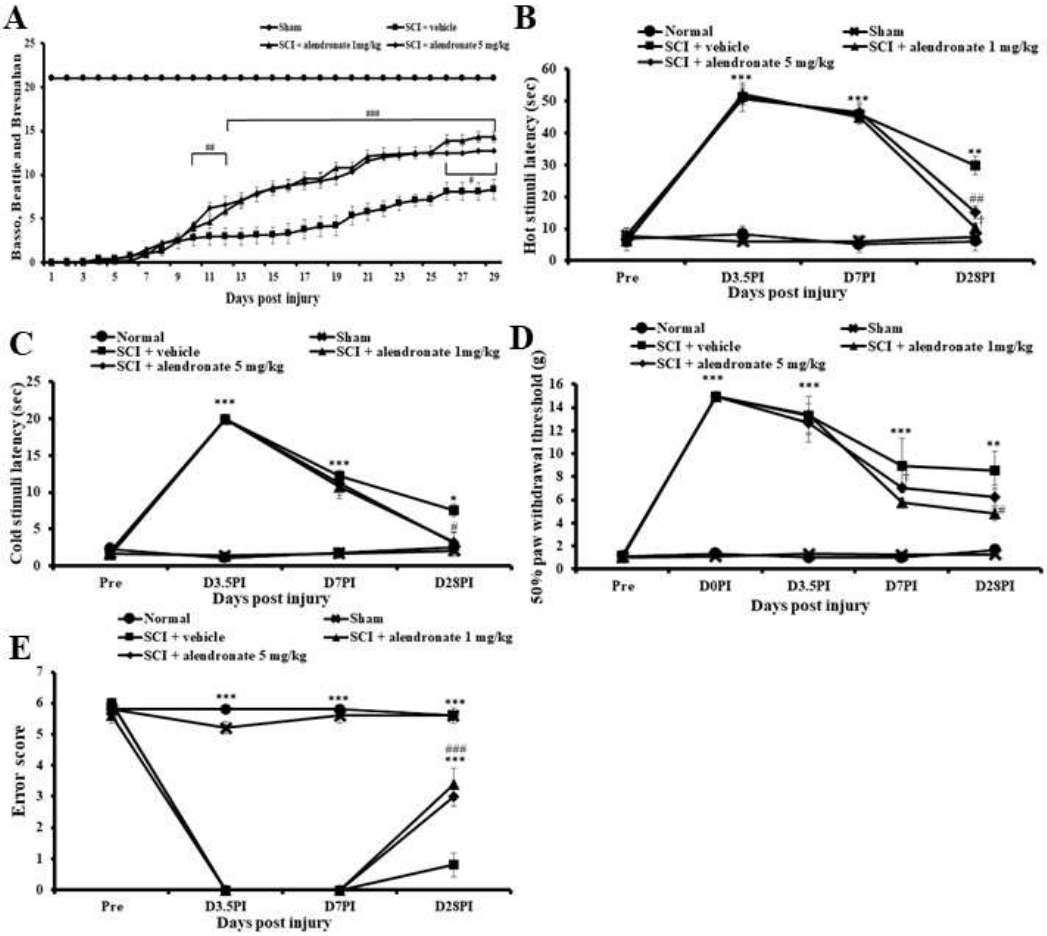

Figure 3. Behavioral assessment. (A) Basso, Beattie, and Bresnahan score. (B) Hot stimuli test. (C) Cold stimuli test. (D) von Frey filament test. (E) Horizontal ladder walking test. *, $p < 0.05$; **, $p < 0.01$; ***, $p < 0.001$ vs. normal. #, $p < 0.05$; ##, $p < 0.01$; ###, $p < 0.001$ vs. spinal cord injury (SCI) + vehicle. †, $p < 0.05$ vs. SCI + alendronate 1 mg/kg.

4.2. Histopathological examination

The histopathological examination was performed using the normal control, the SCI + vehicle-treated group, and the SCI + alendronate 1 mg/kg-treated group. In the core region of the spinal cords of the SCI-induced rats (Fig. 4B and 4C), hemorrhage, vacuolar degeneration and infiltration of inflammatory cells were observed, but in the normal control there were no infiltrated cells (Fig. 4A). A positive immunoreaction to the macrophage marker ED1 was also not detected in the normal control (Fig. 4D), whereas an intense reaction was detected in both the SCI + vehicle-treated group and the SCI + alendronate 1 mg/kg-treated groups (Fig. 4E and 4F). However, the ED1-positive area in SCI + alendronate 1 mg/kg-treated group was significantly smaller than that of the SCI + vehicle-treated group (Fig. 4G).

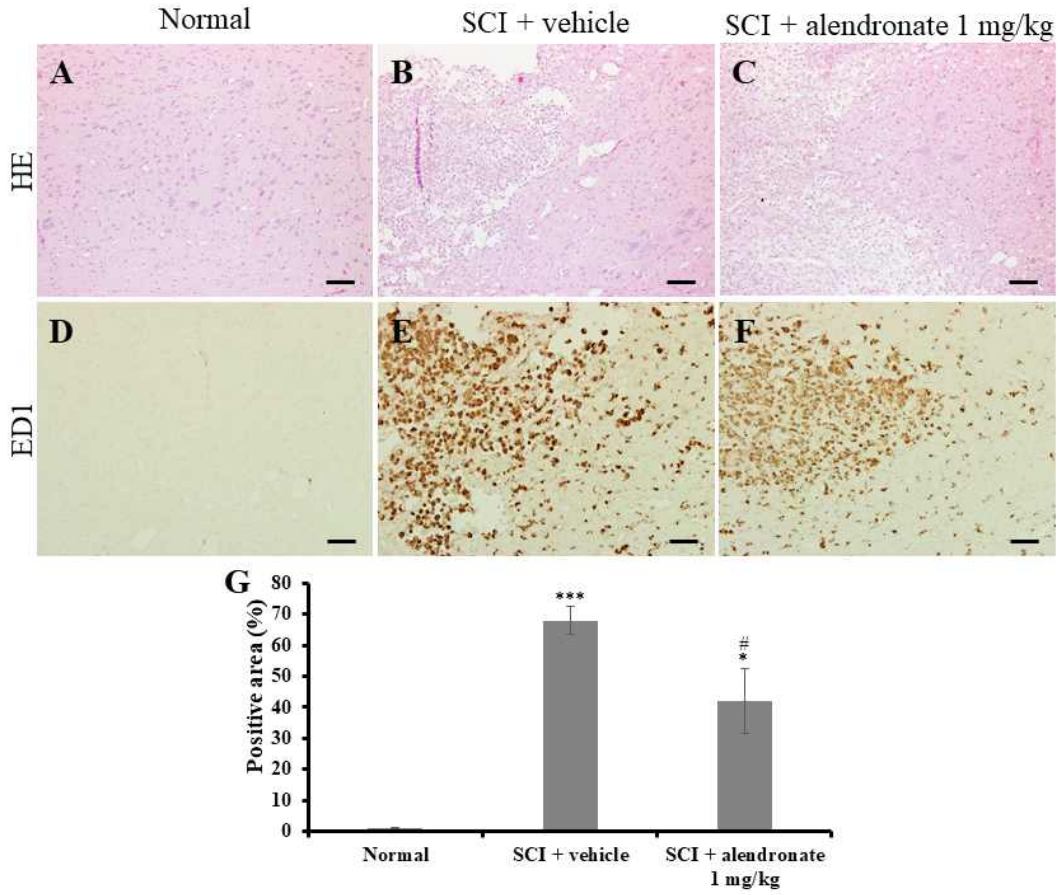

Figure 4. Histopathological evaluation of the spinal cord in normal control and SCI-induced rats. (A–C) Cell infiltration in SCI rats (B and C) normal controls (A). ED1-positive macrophages in the core lesions of the SCI + vehicle-treated group (E) and SCI + alendronate 1 mg/kg-treated group (F). Under alendronate treatment, the size of the ED1-positive area was reduced (G). Scale bars = 50 μm. *, $p < 0.05$; ***, $p < 0.001$ vs. normal. #, $p < 0.05$ vs. SCI + vehicle.

4.3. Alendronate reduced the activation of microglia and astrocytes

The activation of microglia and astrocytes was investigated immunohistochemically using antibodies against ionized calcium-binding adapter molecule 1 (Iba1) and glial fibrillary acidic protein (GFAP). An Iba1-positive immunoreaction was detected in the normal control (Fig. 5A) and in the SCI-induced rats (Fig. 5B and 5C). However, the Iba1-positive area in the SCI + alendronate 1 mg/kg-treated group was significantly smaller than that in the SCI + vehicle-treated group (Fig. 5D). Similarly, a GFAP-positive immunoreaction was detected in the normal control (Fig. 5E) and in SCI-induced rats treated with vehicle (Fig. 5F) or alendronate 1 mg/kg (Fig. 5G), but the GFAP-positivity was significantly less in the SCI + alendronate 1 mg/kg-treated group than in the SCI + vehicle-treated group (Fig. 5H).

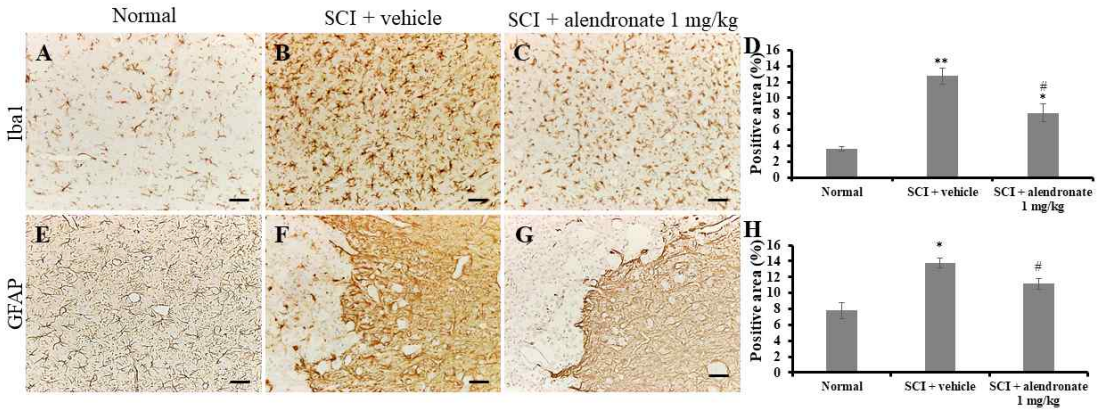

Figure 5. Immunohistochemical analysis of ionized calcium-binding adapter molecule 1 (Iba1) and glial fibrillary acidic protein (GFAP) in normal control and SCI-induced rats. Iba1-positivity in normal (A), SCI + vehicle-treated (B) and SCI + alendronate 1 mg/kg-treated (C) rats. A semi-quantitative analysis showed the reduced activation of microglia in the SCI + alendronate 1 mg/kg-treated group (D). GFAP staining was detected in normal (E), SCI + vehicle-treated (F) and SCI + alendronate 1 mg/kg-treated (G) rats. A semi-quantitative analysis showed a significant decrease in GFAP staining in the SCI + alendronate 1 mg/kg-treated group (H). Scale bars = 50 μm. *, $p < 0.05$; **, $p < 0.01$ vs. normal. #, $p < 0.05$ vs. SCI + vehicle.

4.4. Alendronate relieved the inflammatory responses

MAPK signaling, including ERK1/2 (approximately 44 and 42 kDa), JNK1/2 (approximately 46 and 54 kDa) and p38, and p53, are indicators of neuro-inflammation and are activated in SCI (Kaminska et al., 2009, Martini et al., 2016). At D3.5PI, the ratio of p-ERK2/total ERK2 (2.93 ± 0.45 fold; $p < 0.05$) and p-JNK2/total JNK2 (3.18 ± 0.78 fold; $p < 0.05$) in the SCI + alendronate 1 mg/kg-treated group was down-regulated significantly compared with the ratio in the SCI + vehicle-treated group (3.70 ± 0.37 fold and 4.51 ± 0.92 fold, respectively; Fig. 6A and 6B). In the SCI + vehicle-treated group, p-ERK2/total ERK2 (3.47 ± 0.20 fold; $p < 0.01$), p-JNK1/total JNK1 (2.01 ± 0.11 fold; $p < 0.01$), p-JNK2/total JNK2 (4.52 ± 1.30 fold; $p < 0.05$), and p-p38/total p38 (3.27 ± 0.59 fold; $p < 0.05$) were significantly increased at D7PI, the peak stage of inflammation, compared with the ratios in the normal control (Fig. 6A-C). However, alendronate treatment suppressed the up-regulation of p-JNK1/total JNK1 (1.45 ± 0.16 fold; $p < 0.01$) during the same period (Fig. 6A–C). It also significantly suppressed the increase in the level of p53 protein (1.34 ± 0.07 fold and 1.40 ± 0.15 fold; $p < 0.05$, respectively) at D7PI and D28PI compared to the level in the SCI + vehicle-treated group (1.79 ± 0.01 fold and 2.18 ± 0.21 fold, respectively; Fig. 6D).

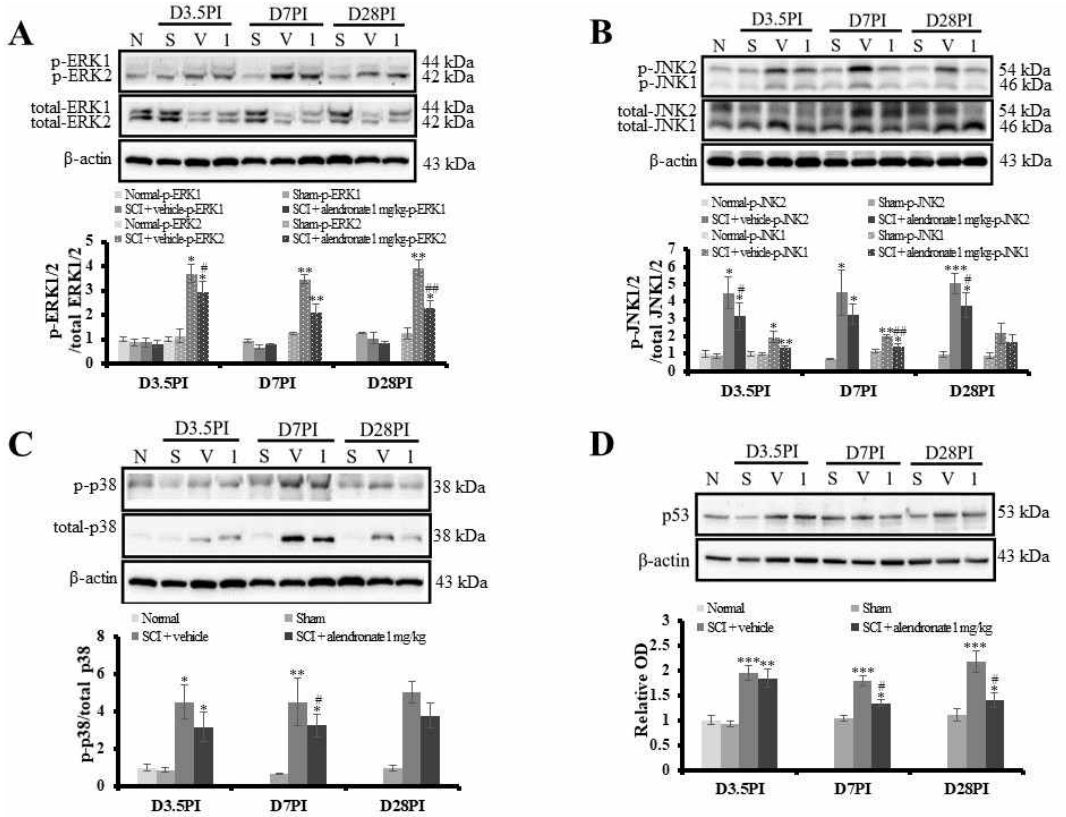

Figure 6. Western blot of mitogen-activated protein kinase (MAPK) signaling and p53. Representative immunoblots of phosphorylated extracellular signal-regulated kinase1/2 (p-ERK1/2; ~44 and ~42 kDa) (A), c-jun-NH_2-terminal kinase1/2 (p-JNK1/2; ~46 and ~54 kDa) (B), and phosphorylated p38 (p-p38; ~38 kDa) (C), and p53 (D). The expression levels of p-ERK2/total ERK2 (A), p-JNK1/2/total JNK1/2 (B), and p-p38/total p38 (C) in the SCI + alendronate 1 mg/kg-treated group decreased significantly compared with the SCI + vehicle-treated group. The level of p53 protein was also significantly reduced (D) compared with the SCI + vehicle group. *, $p < 0.05$; **, $p < 0.01$; ***, $p < 0.001$ vs. normal. #, $p < 0.05$; ##, $p < 0.01$ vs. SCI + vehicle.

A quantitative real time-PCR was performed to measure the levels of several pro-inflammatory cytokines and pro-inflammatory mediators. The mRNA expression levels of pro-inflammatory cytokines, including IL-1β (Fig. 7A) and TNF-α (Fig. 7B) were significantly up-regulated in the SCI + vehicle-treated group ($p < 0.01$ and $p < 0.05$, respectively vs. the normal control). By contrast, alendronate significantly inhibited the up-regulation of IL-1β and TNF-α mRNA in the SCI + alendronate 1 mg/kg-treated group ($p < 0.05$, respectively; Fig. 7A and 7B). In addition, the mRNA levels of the pro-inflammatory mediators, cyclooxygenase-2 (COX-2) and Serpina3n, were significantly increased in the SCI + vehicle-treated group ($p < 0.05$ and $p < 0.001$, respectively vs. normal control; Fig. 7C and 7D). However, alendronate treatment did not inhibit the increase in COX-2 mRNA (Fig. 7C) but it did down-regulate the levels of Serpina3n mRNA (Fig. 7D).

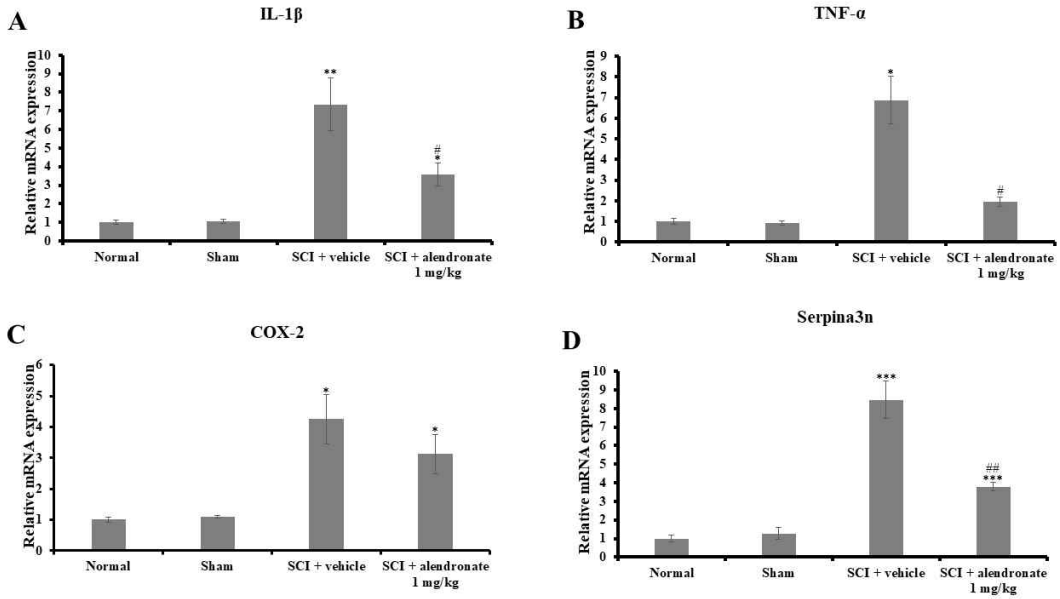

Figure 7. Analysis of pro-inflammatory responses in normal and SCI-induced rats. The levels of the pro-inflammatory cytokines, interleukin-1 beta (IL-1β) (A) and tumor necrosis factor-alpha (TNF-α) (B), increased significantly in the SCI + vehicle-treated group but were significantly reduced by alendronate treatment. Under SCI, the expression levels of the pro-inflammatory mediators, cyclooxygenase-2 (COX-2) (C) and serine peptidase inhibitor, clade A, member 3N (Serpina3n) were significantly increased (D). Alendronate treatment did not suppress the increase in the COX-2 mRNA level (C) but it did prevent the up-regulation of Serpina3n expression (D). *, $p < 0.05$; **, $p < 0.01$; ***, $p < 0.01$ vs. normal. #, $p < 0.05$; ##, $p < 0.01$ vs. SCI + vehicle.

4.5. Alendronate promoted the axonal regeneration

Immunohistochemical staining was conducted using the calcitonin gene-related peptide (CGRP), choline acetyltransferase (ChAT), and potassium chloride co-transporter 2 (KCC2), representative markers for axonal regeneration (Kim et al., 2018, Kosaka et al., 2020). In the SCI groups, CGRP-positivity on D7PI (Fig. 8B and 8C) and D28PI (Fig. 8E and 8F) was higher than in the normal control (Fig. 8A and 8D, respectively). In the alendronate-treated groups, the level of CGRP up-regulated differed significantly from the normal control on D7PI to D28PI ($p < 0.05$, Fig. 8G). However, CGRP-positivity in the SCI + vehicle-treated group was higher than in the normal control on D28PI ($p < 0.05$, Fig. 8G). ChAT staining was localized in neurons of the normal controls on D7PI and D28PI (Fig. 8H and 8K, respectively) whereas it was significantly decreased ($p < 0.05$, Fig. 8N) in both the SCI + vehicle-treated group (Fig. 8I) and the SCI + alendronate 1 mg/kg-treated group (Fig. 8J) at D7PI. However, compared to the SCI + vehicle-treated group, ChAT-positivity markedly increased in the SCI + alendronate 1 mg/kg-treated group ($p < 0.01$) on D28PI (Fig. 8L-N). KCC2 expression decreased significantly in the SCI + vehicle-treated group (Fig. 8P, 8S, and 8U), but not in the SCI + alendronate 1 mg/kg-treated group (Fig. 8Q, 8T, and 8U) on D7PI and D28PI. Alendronate treatment restored the expression level of KCC2 to that of the normal control (Fig. 8A). These results suggested that alendronate promotes axonal regeneration after SCI.

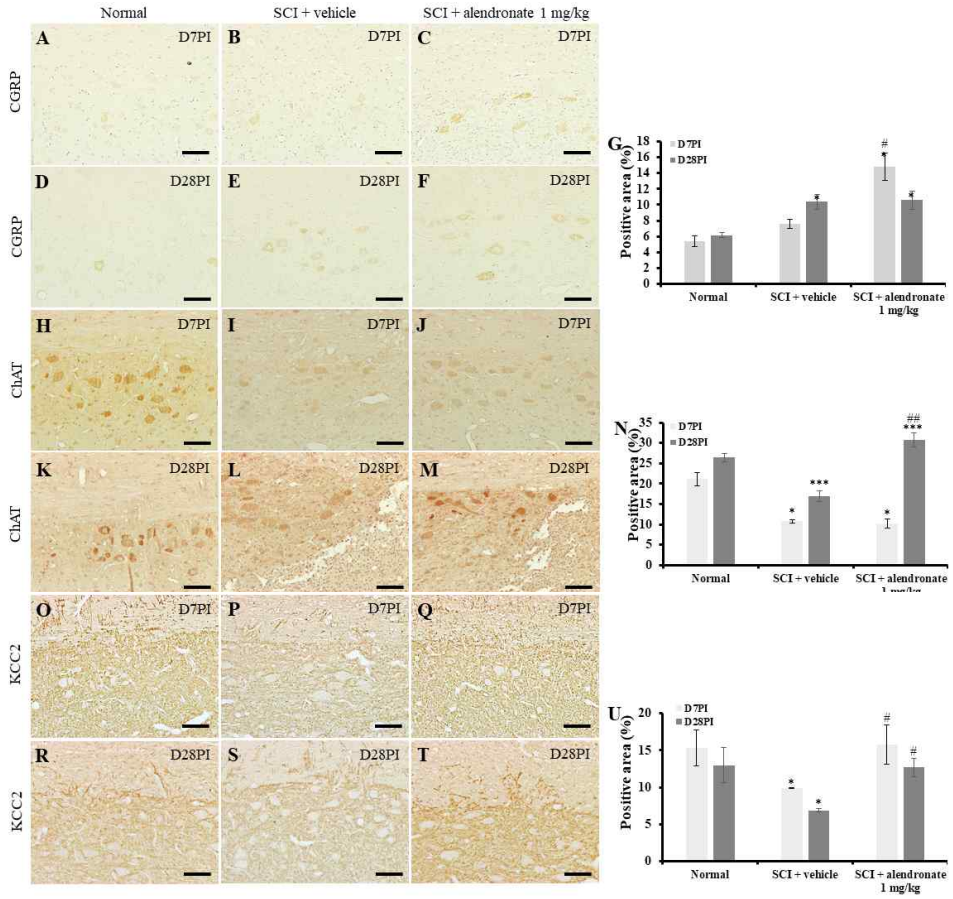

Figure 8. Immunohistochemical evaluation of calcitonin gene-related peptide (CGRP), choline acetyltransferase (ChAT), and potassium chloride co-transporter 2 (KCC2) in normal control and SCI-induced rats. CGRP was detected in the motor neurons of normal (A and D), SCI + vehicle-treated (B and E) and SCI + alendronate 1 mg/kg-treated (C and F) rats and was increased in the SCI + alendronate 1 mg/kg-treated group (G) at D7PI. In the motor neurons of the SCI + vehicle-treated group and SCI + alendronate 1 mg/kg-treated group the levels increased significantly at D28PI (G). ChAT was detected in the motor neurons of normal control rats (H and K) but not in the SCI + vehicle-treated group (I) or in the SCI + alendronate 1 mg/kg-treated group (J) at D7PI (N). A semi-quantitative

analysis indicated a sharp increase in ChAT levels in the SCI + alendronate 1 mg/kg-treated group (L) but not in the SCI + vehicle-treated group (M) at D28PI (N). KCC2-positive foci were detected around the neurons of normal control (O and R), SCI + vehicle-treated (P and S) and SCI + alendronate 1 mg/kg-treated (Q and T) rats. Alendronate treatment inhibited the down-regulation of KCC2 (U). Scale bars = 100 μm. *, $p < 0.05$; ***, $p < 0.001$ vs. normal. #, $p < 0.05$, ##, $p < 0.01$ vs. SCI + vehicle.

5. Discussion

This is the first study to show that alendronate, a nitrogen-containing bisphosphonate, suppresses inflammatory responses associated with SCI, including the up-regulation of pro-inflammatory cytokines, inflammatory mediators and the infiltration of inflammatory cells and the activation of microglia/astrocytes. Our results showed that, in an animal model of SCI characterized by severe inflammation, gliosis, and sensorimotor dysfunction, alendronate promotes the axonal regeneration by restoring the expression of CGRP, ChAT and KCC2 to normal levels.

Bisphosphonate drugs have been classified as non-nitrogen- and nitrogen-containing bisphosphonates based on their molecular structure (Panagiotakou et al., 2020). Alendronate is a nitrogen-containing bisphosphonate. The action of nitrogen-containing bisphosphonates involves the mevalonate pathway and inhibition of farnesyl-pyrophosphate synthase (Panagiotakou et al., 2020). Farnesyl-pyrophosphate synthase suppression modifies GTPase so that the osteoclast cytoskeleton is affected (Panagiotakou et al., 2020). The effect of alendronate on osteoporosis has been evaluated in ovariectomized rats, where it was shown to promote the healing of osteoporotic fractures (Zhang et al., 2020).

Alendronate improved the learning and memory in a mouse model of Alzheimer's disease by decreasing neuro-inflammation, oxidative stress, and the Aβ1-42 deposition induced by an intracerebroventricular streptozotocin infusion (Zameer et al., 2019). The improvement in Alzheimer's disease in response to alendronate has been shown to result from a significant decrease in Aβ1-42 and β-site amyloid precursor protein cleaving enzyme-1, a key marker of Alzheimer's disease (Zameer et al., 2019). In

neurodegenerative disease, such as experimental autoimmune encephalomyelitis, alendronate mitigates hind-limb paralysis, suppresses T cell proliferation, and limits the inflammatory response (Jung et al., 2020). Therefore, this result suggests that alendronate ameliorates the severe inflammation in SCI rats.

SCI can be divided into an early inflammatory stage (~D3PI), a cleaning stage (D4PI–D14PI), and a reactive gliosis stage (D14PI~) and includes apoptosis and necrosis (Shin et al., 2013). To study the inflammatory response, we examined the expression of ED1, Iba1, and GFAP, representative of infiltrated inflammatory cells, microglia and astrocytes, respectively. Our results showed that the infiltration of inflammatory cells and activation of microglia/astrocytes were repressed by alendronate treatment.

As mediators of the inflammatory response, the levels of MAPK signaling, p53, IL-1β, TNF-α, COX-2 and Serpina3n were determined. The key molecules in MAPK signaling are ERK1/2, JNK1/2 and p38 (Martini et al., 2016). MAPK signaling activation, via phosphorylation (Cargnello and Roux, 2011), contributes to central nervous system inflammation (Kaminska et al., 2009). A previous study showed that the inhibition of MAPK signaling improved the behavioral dysfunction induced by SCI, by blocking apoptosis (Martini et al., 2016). In a rat model of osteoporosis, alendronate reduced the number of apoptotic cells and inflammation by targeting adenylyl cyclase isoform 6, through the regulation of MAPK signaling, including ERK and p38 (Pan et al., 2018). MAPK signaling inhibition also alleviates inflammation via the down-regulation of pro-inflammatory cytokines, including IL-1β and TNF-α (Bachstetter and

Van Eldik, 2010). Phosphorylated p38 plays a critical role in the activation of p53 provoked by chemotherapy (Sanchez-Prieto et al., 2000). The blockade of p38 inhibits the transcriptional activity of p53 by negatively regulating cell proliferation and mediating the death of highly damaged cells (Floriddia et al., 2012). The increased p38 sequentially promotes p53 (Sanchez-Prieto et al., 2000) and pro-inflammatory cytokines, IL-1β and TNF-α (Kasuya et al., 2018). In our study, p53 and p38 expression increased during the early inflammatory stage, with significant differences between the SCI + vehicle-treated group and the SCI + alendronate 1 mg/kg-treated group on D7PI. These results provided further evidence that alendronate treatment alleviates inflammation after SCI via down-regulation of MAPK signaling and p53.

Serpina3n is a member of the serpin superfamily, which encodes anti-chymotrypsin and key molecules involved in the inflammatory response in the brain (Abraham, 2001) and in high-fat-diet-induced hypothalamic neuro-inflammation (Abcouwer et al., 2013). The over-expression of Serpina3n in the hippocampus blocks the anti-inflammatory effect of melatonin on trimethyltin chloride-induced neurotoxicity (Xi et al., 2019). An increase in Serpina3n levels in active astrocytes has also been reported (Zamanian et al., 2012). In our study, the up-regulated Serpina3n was suppressed by alendronate treatment, consistent with the drug's anti-inflammatory effect. This result suggested that Serpina3n plays a pivotal role in SCI-induced neuro-inflammation and is a crucial target of alendronate in its relief of SCI-induced neuro-inflammation.

In addition to the inflammatory response, SCI is characterized by behavioral dysfunctions due to axon damage (Egawa et al., 2017). The

neuropeptide CGRP, is synthesized in the dorsal root ganglion and ventral horn of the spinal cord at high concentrations (Mulderry et al., 1985). Under normal conditions, CGRP is transported to the axon terminals of sensory nerve fibers (Zhang et al., 2016) but its levels transiently increase in response to axonal injury induced by SCI (Weaver et al., 2001), facial nerve injury (Kim et al., 2018), and tibial nerve injury (Kosaka et al., 2020). An increase in CGRP also occurs when motor neurons of the CNS are injured, in parallel with up-regulated glial cell line derived neurotrophic factor (Blesch and Tuszynski, 2001). It is therefore likely that alendronate treatment led to an accelerated up-regulation of CGRP, an increase of which acts to restore damaged axons.

The enzyme ChAT catalyzes the synthesis of acetylcholine, a brain neurotransmitter (Kumar et al., 2017) and a marker of motor neuron regeneration used in peripheral nerve injury models, including hypoglossal nerve injury (Tatetsu et al., 2012) and facial nerve injury (Kim et al., 2018). The inhibition or down-regulation of ChAT, and thus the depression of acetylcholine production, in injured motor neurons are seen in the early stage after axotomy, but the level gradually recovers to normal during axonal regeneration (Tatetsu et al., 2012, Kim et al., 2018 and Kosaka et al., 2020), thus restoring neural signal transduction (Lu et al., 2012). In the present study, of ChAT expression ceased at D7PI after SCI but resumed at D28PI under alendronate treatment, thus demonstrating that alendronate treatment contributes to axonal regeneration.

KCC2 is responsible for balancing the chloride ion gradient in the central nervous system (Chamma et al., 2012). Its down-regulation of KCC2 is observed in SCI (Boulenguez et al., 2010) and peripheral nerve

injuries, including those involving the hypoglossal nerve (Tatetsu et al., 2012), facial nerve (Kim et al., 2018), and tibial nerve (Kosaka et al., 2020). The imbalance in the intracellular chloride ion concentration that follows a decrease in KCC2 levels induces a shift from gamma-aminobutytic acid/glycine inhibition to excitation in post-synaptic neurons (Kim et al., 2018) and promotes axonal regeneration after injury (Tatetsu et al., 2012, Kim et al., 2018 and Kosaka et al., 2020). During axonal degeneration and regeneration, the restoration of KCC2 levels is accompanied by behavioral and functional recovery both after facial nerve injury (Kim et al., 2018) and tibial nerve injury (Kosaka et al., 2020). Alendronate treatment may therefore allow a gradual recovery of KCC2 and, thus, behavioral improvements through the early onset of axonal regeneration.

In conclusion, our study showed that the anti-inflammatory properties of alendronate in an animal model of SCI include the reduced infiltration of inflammatory cells and an alleviation of inflammatory responses, including microgliosis/astrogliosis. Alendronate also enhanced axonal regeneration. Based on its demonstrated effects in rats, alendronate treatment may contribute to the functional recovery of SCI in humans (Fig. 9).

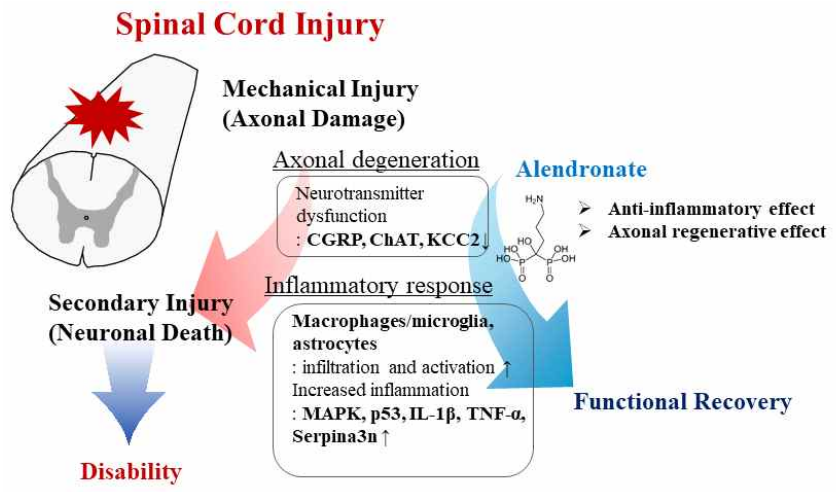

Figure 9. Summary of the therapeutic effects of alendronate in SCI. Alendronate treatment ameliorated secondary injury in SCI rats by suppressing inflammation and promoting axonal regeneration, in turn, leading to functional recovery. CGRP, calcitonin gene-related peptide; ChAT, choline acetyltransferase; IL-1β, interleukin-1 beta; KCC2, potassium chloride co-transporter 2; Serpina3n, serin peptidase inhibitor, clade A, member 3N; TNF-α, tumor necrosis factor-alpha.

References

Abcouwer, S.F., Lin, C.M., Shanmugam, S., Muthusamy, A., Barber, A.J., Antonetti, D.A., 2013. Minocycline prevents retinal inflammation and vascular permeability following ischemia-reperfusion injury. J Neuroinflammation 10, 149.

Abraham, C.R., 2001. Reactive astrocytes and alpha1-antichymotrypsin in Alzheimer's disease. Neurobiol Aging 22, 931-936.

Ahmed, R.U., Alam, M., Zheng, Y.P., 2019. Experimental spinal cord injury and behavioral tests in laboratory rats. Heliyon 5, e01324.

Ahn, M., Lee, C., Jung, K., Kim, H., Moon, C., Sim, K.B., Shin, T., 2012. Immunohistochemical study of arginase-1 in the spinal cords of rats with clip compression injury. Brain Res 1445, 11-19.

Bachstetter, A.D., Van Eldik, L.J., 2010. The p38 MAP Kinase Family as Regulators of Proinflammatory Cytokine Production in Degenerative Diseases of the CNS. Aging Dis 1, 199-211.

Basso, D.M., Beattie, M.S., Bresnahan, J.C., 1995. A sensitive and reliable locomotor rating scale for open field testing in rats. J Neurotrauma 12, 1-21.

Blesch, A., Tuszynski, M.H., 2001. GDNF gene delivery to injured adult CNS motor neurons promotes axonal growth, expression of the trophic neuropeptide CGRP, and cellular protection. J Comp Neurol 436, 399-410.

Boulenguez, P., Liabeuf, S., Bos, R., Bras, H., Jean-Xavier, C., Brocard, C., Stil, A., Darbon, P., Cattaert, D., Delpire, E., Marsala, M., Vinay, L., 2010. Down-regulation of the potassium-chloride cotransporter KCC2 contributes to spasticity after spinal cord injury. Nat Med 16, 302-307.

Cargnello, M., Roux, P.P., 2011. Activation and function of the MAPKs and their substrates, the MAPK-activated protein kinases. Microbiol Mol Biol Rev 75, 50-83.

Chamma, I., Chevy, Q., Poncer, J.C., Levi, S., 2012. Role of the neuronal K-Cl co-transporter KCC2 in inhibitory and excitatory neurotransmission. Front Cell Neurosci 6, 5.

Choi, Y., Oh, H., Ahn, M., Kang, T., Chun, J., Shin, T., Kim, J., 2020. Immunohistochemical analysis of periostin in the hearts of Lewis rats with experimental autoimmune myocarditis. J Vet Med Sci 82, 1545-1550.

Deuis, J.R., Dvorakova, L.S., Vetter, I., 2017. Methods Used to Evaluate Pain Behaviors in Rodents. Front Mol Neurosci 10, 284.

Egawa, N., Lok, J., Washida, K., Arai, K., 2017. Mechanisms of Axonal Damage and Repair after Central Nervous System Injury. Transl Stroke Res 8, 14-21.

Floriddia, E.M., Rathore, K.I., Tedeschi, A., Quadrato, G., Wuttke, A., Lueckmann, J.M., Kigerl, K.A., Popovich, P.G., Giovanni, S.D., 2012. p53 Regulates the neuronal intrinsic and extrinsic responses affecting the recovery of motor function following spinal cord injury. J Neurosci 32, 13956-13970.

Gale, K., Kerasidis, H., Wrathall, J.R., 1985. Spinal cord contusion in the rat: behavioral analysis of functional neurologic impairment. Exp Neurol 88, 123-134.

Gonzalez-Cano, R., Boivin, B., Bullock, D., Cornelissen, L., Andrews, N., Costigan, M., 2018. Up-Down Reader: An Open Source Program for Efficiently Processing 50% von Frey Thresholds. Front Pharmacol 9, 433.

Griffin, J.M., Bradke, F., 2020. Therapeutic repair for spinal cord injury: combinatory approaches to address a multifaceted problem. EMBO

Mol Med 12, e11505.

Heo, S.D., Kim, J., Choi, Y., Ekanayake, P., Ahn, M., Shin, T., 2020. Hesperidin improves motor disability in rat spinal cord injury through anti-inflammatory and antioxidant mechanism via Nrf-2/HO-1 pathway. Neurosci Lett 715, 134619.

Inquimbert, P., Moll, M., Latremoliere, A., Tong, C.K., Whang, J., Sheehan, G.F., Smith, B.M., Korb, E., Athie, M.C.P., Babaniyi, O., Ghasemlou, N., Yanagawa, Y., Allis, C.D., Hof, P.R., Scholz, J., 2018. NMDA Receptor Activation Underlies the Loss of Spinal Dorsal Horn Neurons and the Transition to Persistent Pain after Peripheral Nerve Injury. Cell Rep 23, 2678-2689.

Jung, K., Kim, J., Ahn, G., Matsuda, H., Akane, T., Ahn, M., Shin, T., 2020. Alendronate alleviates the symptoms of experimental autoimmune encephalomyelitis. Int Immunopharmacol 84, 106534.

Kami, K., Taguchi Ms, S., Tajima, F., Senba, E., 2016. Improvements in impaired GABA and GAD65/67 production in the spinal dorsal horn contribute to exercise-induced hypoalgesia in a mouse model of neuropathic pain. Mol Pain 12.

Kaminska, B., Gozdz, A., Zawadzka, M., Ellert-Miklaszewska, A., Lipko, M., 2009. MAPK signal transduction underlying brain inflammation

and gliosis as therapeutic target. Anat Rec (Hoboken) 292, 1902-1913.

Kasuya, Y., Umezawa, H., Hatano, M., 2018. Stress-Activated Protein Kinases in Spinal Cord Injury: Focus on Roles of p38. Int J Mol Sci 19.

Kim, D.H., Heo, S.D., Ahn, M.J., Sim, K.B., Shin, T.K., 2003. Activation of embryonic intermediate filaments contributes to glial scar formation after spinal cord injury in rats. J Vet Sci 4, 109-112.

Kim, J., Kobayashi, S., Shimizu-Okabe, C., Okabe, A., Moon, C., Shin, T., Takayama, C., 2018. Changes in the expression and localization of signaling molecules in mouse facial motor neurons during regeneration of facial nerves. J Chem Neuroanat 88, 13-21.

Kjell, J., Olson, L., 2016. Rat models of spinal cord injury: from pathology to potential therapies. Dis Model Mech 9, 1125-1137.

Kosaka, Y., Yafuso, T., Shimizu-Okabe, C., Kim, J., Kobayashi, S., Okura, N., Ando, H., Okabe, A., Takayama, C., 2020. Development and persistence of neuropathic pain through microglial activation and KCC2 decreasing after mouse tibial nerve injury. Brain Res 1733, 146718.

Kumar, R., Kumar, A., Langstrom, B., Darreh-Shori, T., 2017. Discovery of novel choline acetyltransferase inhibitors using structure-based virtual screening. Sci Rep 7, 16287.

Lu, P., Wang, Y., Graham, L., McHale, K., Gao, M., Wu, D., Brock, J., Blesch, A., Rosenzweig, E.S., Havton, L.A., Zheng, B., Conner, J.M., Marsala, M., Tuszynski, M.H., 2012. Long-distance growth and connectivity of neural stem cells after severe spinal cord injury. Cell 150, 1264-1273.

Martini, A.C., Forner, S., Koepp, J., Rae, G.A., 2016. Inhibition of spinal c-Jun-NH2-terminal kinase (JNK) improves locomotor activity of spinal cord injured rats. Neurosci Lett 621, 54-61.

Metz, G.A., Whishaw, I.Q., 2002. Cortical and subcortical lesions impair skilled walking in the ladder rung walking test: a new task to evaluate fore- and hindlimb stepping, placing, and co-ordination. J Neurosci Methods 115, 169-179.

Moore, K.A., Kohno, T., Karchewski, L.A., Scholz, J., Baba, H., Woolf, C.J., 2002. Partial peripheral nerve injury promotes a selective loss of GABAergic inhibition in the superficial dorsal horn of the spinal cord. J Neurosci 22, 6724-6731.

Mulderry, P.K., Ghatei, M.A., Bishop, A.E., Allen, Y.S., Polak, J.M., Bloom, S.R., 1985. Distribution and chromatographic characterisation of CGRP-like immunoreactivity in the brain and gut of the rat. Regul Pept 12, 133-143.

Nishii, T., Tamura, S., Shiomi, T., Yoshikawa, H., Sugano, N., 2013. Alendronate treatment for hip osteoarthritis: prospective randomized 2-year trial. Clin Rheumatol 32, 1759-1766.

Oliveira, J.R., Oliveira, M.F., 2016. Primary brain calcification in patients undergoing treatment with the biphosphanate alendronate. Sci Rep 6, 22961.

Pan, B.L., Tong, Z.W., Li, S.D., Wu, L., Liao, J.L., Yang, Y.X., Li, H.H., Dai, Y.J., Li, J.E., Li, P., 2018. Decreased microRNA-182-5p helps alendronate promote osteoblast proliferation and differentiation in osteoporosis via the Rap1/MAPK pathway. Biosci Rep 38.

Panagiotakou, A., Yavropoulou, M., Nasiri-Ansari, N., Makras, P., Basdra, E.K., Papavassiliou, A.G., Kassi, E.V., 2020. Extra-skeletal effects of bisphosphonates. Metabolism 110, 154264.

Sanchez-Prieto, R., Rojas, J.M., Taya, Y., Gutkind, J.S., 2000. A role for the p38 mitogen-acitvated protein kinase pathway in the

transcriptional activation of p53 on genotoxic stress by chemotherapeutic agents. Cancer Res 60, 2464-2472.

Sharpe, M., Noble, S., Spencer, C.M., 2001. Alendronate: an update of its use in osteoporosis. Drugs 61, 999-1039.

Shin, T., Ahn, M., Moon, C., Kim, S., Sim, K.B., 2013. Alternatively activated macrophages in spinal cord injury and remission: another mechanism for repair? Mol Neurobiol 47, 1011-1019.

Tatetsu, M., Kim, J., Kina, S., Sunakawa, H., Takayama, C., 2012. GABA/glycine signaling during degeneration and regeneration of mouse hypoglossal nerves. Brain Res 1446, 22-33.

Tran, T.S., Alijani, A., Phelps, P.E., 2003. Unique developmental patterns of GABAergic neurons in rat spinal cord. J Comp Neurol 456, 112-126.

Tricarico, P.M., Girardelli, M., Kleiner, G., Knowles, A., Valencic, E., Crovella, S., Marcuzzi, A., 2015. Alendronate, a double-edged sword acting in the mevalonate pathway. Mol Med Rep 12, 4238-4242.

Weaver, L.C., Verghese, P., Bruce, J.C., Fehlings, M.G., Krenz, N.R., Marsh, D.R., 2001. Autonomic dysreflexia and primary afferent sprouting after clip-compression injury of the rat spinal cord. J

Neurotrauma 18, 1107-1119.

Xi, Y., Liu, M., Xu, S., Hong, H., Chen, M., Tian, L., Xie, J., Deng, P., Zhou, C., Zhang L., He, M., Chen, C., Lu, Y., Reiter, R., Yu, Z., Pi, H., Zhou, Z., 2019. Inhibition of SERPINA3N-dependent neuroinflammation is essential for melatonin to ameliorate trimethyltin chloride-induced neurotoxicity. J Pineal Res 67, e12596.

Yao, Y., Tan, Y.H., Light, A.R., Mao, J., Yu, A.C., Fu, K.Y., 2016. Alendronate Attenuates Spinal Microglial Activation and Neuropathic Pain. J Pain 17, 889-903.

Zamanian, J.L., Xu, L., Foo, L.C., Nouri, N., Zhou, L., Giffard, R.G., Barres, B.A., 2012. Genomic analysis of reactive astrogliosis. J Neurosci 32, 6391-6410.

Zameer, S., Kaundal, M., Vohora, D., Ali, J., Kalam Najmi, A., Akhtar, M., 2019. Ameliorative effect of alendronate against intracerebroventricular streptozotocin induced alteration in neurobehavioral, neuroinflammation and biochemical parameters with emphasis on Abeta and BACE-1. Neurotoxicology 70, 122-134.

Zameer, S., Najmi, A.K., Vohora, D., Akhtar, M., 2018. Bisphosphonates: Future perspective for neurological disorders. Pharmacol Rep 70, 900-907.

Zhang, C., Zhu, J., Jia, J., Guan, Z., Sun, T., Zhang, W., Yuan, W., Wang, H., Leng, H., Song, C., 2020. Once-weekly parathyroid hormone combined with ongoing long-term alendronate treatment promotes osteoporotic fracture healing in ovariectomized rats. J Orthop Res.

Zhang, Y., Yang, J., Zhang, P., Liu, T., Xu, J., Fan, Z., Shen, Y., Li, W., Zhang, H., 2016. Calcitonin gene-related peptide is a key factor in the homing of transplanted human MSCs to sites of spinal cord injury. Sci Rep 6, 27724.

Abstract in Korean

척수손상모델에서 alendronate의 치료 효과

(지도교수 : 신 태 균)

최 유 나

제주대학교 일반대학원 수의학과

척수손상은 교통사고와 같은 외상을 포함하여 다양한 원인에 의해 발생하며 손상 부위에 출혈 및 중추신경계 구성 세포 특히 신경세포의 사멸로 인한 신경 염증이 주요 소견이다. 더불어, 척수손상모델에서 산화적 손상과 염증 매개 물질의 증가를 포함한 염증 반응이 이차 손상의 특징을 나타내므로, 치료를 위해 항산화물질 또는 항염증물질이 사용되고 있다. 따라서, 본 연구에서는 골다공증 치료약물인 alendronate가 척수손상모델에서 어떠한 효과를 나타내는지 평가하였다. Alendronate는 수술 시행일부터 조직 채취일까지 하루에 한 번 1, 5 mg/kg의 농도로 복강내 투여하였다. 운동기능 평가를 위해 Basso, Beattie and Bresnahan scoring, 감각기능 평가를 위해 hot and cold stimuli test와 von Frey filament test, 운동/감각기능 평가를 위해 horizontal ladder walking test를 실시하였으며, alendronate 처리군에서 비처리군에 비해 운동 및 감각 기능 개선효과를 확인하였다. 조직학적평가를 통해 염증세포의 침윤과 microgliosis/astrogliosis를 포함한 척수 조직 내 염증 반응이 alendronate에 의해 완화된 것을 확인하였다. 또한 Western blot analysis와 real time PCR로 pro-inflammatory cytokine과 pro-inflammatory mediator의 발현량 차이를 확인한 결과, 비처리군에 비해 alendronate

치료군에서 유의성 있게 감소하였음을 검증하였다. 더불어, calcitonin gene-related peptide, choline acetyltransferase, potassium chloride co-transporter 2를 이용한 면역조직화학염색을 통해 alendronate 처리군에서 축삭재생 촉진 효과를 검증하였다. 본 연구는 척수 손상 후 발생하는 이차적 손상인 염증 반응이 alendronate 투여에 의해 억제가 되며, 손상된 신경세포의 축삭 재생을 촉진시켰으며 이는 운동 및 감각기능이 개선되었음을 처음으로 확인한 결과이다.

주요어: Alendronate, 축삭 재생, 행동검사, 염증, 척수 손상